A preliminary version of this manuscript has been presented at the
5th International Symposium on Solar Sailing, (29 July – 2 August 2019, Aachen, Germany).

Optimal Solar Sail Trajectory Approximation with Finite Fourier Series

Andrea Caruso*, Marco Bassetto, Giovanni Mengali, Alessandro A. Quarta

Department of Civil and Industrial Engineering, University of Pisa, I-56122 Pisa, Italy

Abstract

The heliocentric transfer of a solar sail-based spacecraft is usually studied from an optimal perspective, by looking for the control law that minimizes the total flight time. The optimal control problem can be solved either with an indirect approach, whose solution is difficult to obtain due to its sensitivity to an initial guess of the costates, or with a direct method, which requires a good estimate of a feasible (guess) trajectory. This work presents a procedure to generate an approximate optimal trajectory through a finite Fourier series. The minimum time problem is solved using a nonlinear programming solver, in which the optimization parameters are the coefficients of the Fourier series and the positions of the spacecraft along the initial and target orbits. Suitable constraints are enforced on the direction and magnitude of the sail propulsive acceleration vector in order to obtain feasible solutions. A comparison with the numerical results from an indirect approach shows that the proposed method provides a good approximation of the optimal trajectory with a small computational effort.

Keywords: Solar sail trajectory optimization, Finite Fourier series, Shape-based method

Nomenclature

$\boldsymbol{a}$	=	propulsive acceleration vector, $[\mathrm{mm/s^2}]$
$\{a_r, a_\theta, a_\phi\}$	=	propulsive acceleration components in $\mathcal{T}_s$, $[\mathrm{mm/s^2}]$
a	=	semimajor axis, [au]
a_c	=	characteristic acceleration, $[\mathrm{mm/s^2}]$
$a_\oplus$	=	Sun's gravitational acceleration at $r = 1\,\mathrm{au}$, $[\mathrm{mm/s^2}]$
$\{a_0, a_1, a_2\}$	=	auxiliary coefficients
$\{b_1, b_2, b_3\}$	=	sail force coefficients
$\{b_{fn}, c_{fn}\}$	=	Fourier series coefficients
e	=	orbital eccentricity
$\{\hat{\boldsymbol{e}}_r, \hat{\boldsymbol{e}}_\theta, \hat{\boldsymbol{e}}_\phi\}$	=	unit vectors of $\mathcal{T}_s$ reference frame
f	=	Fourier series expression
i	=	orbital inclination, [deg]
N_c	=	number of Fourier series coefficients
N_p	=	number of nodes
N_u	=	number of control variables
$\hat{\boldsymbol{n}}$	=	normal unit vector
O	=	Sun's center-of-mass
p	=	semilatus rectum, [au]

*Corresponding author
Email addresses: andrea.caruso@ing.unipi.it (Andrea Caruso), marco.bassetto@ing.unipi.it (Marco Bassetto), g.mengali@ing.unipi.it (Giovanni Mengali), a.quarta@ing.unipi.it (Alessandro A. Quarta)

Published in Advances in Space Research, Vol. 67, No. 9, May 2021, pp. 2834–2843. doi: https://doi.org/10.1016/j.asr.2019.11.019

$\{q_1, q_2\}$	=	auxiliary coefficients
$\boldsymbol{r}$	=	position vector, [au]
r	=	Sun-spacecraft distance, [au]
s	=	auxiliary variable
t	=	time, [days]
t_f	=	total time of flight, [days]
$\mathcal{T}_\epsilon(O; x_\epsilon, y_\epsilon, z_\epsilon)$	=	heliocentric-ecliptic reference frame
$\mathcal{T}_s(O; r, \theta, \phi)$	=	spherical reference frame
$\{v_r, v_\theta, v_\phi\}$	=	velocity components in $\mathcal{T}_s$, [km/s]
$\{v_{\epsilon x}, v_{\epsilon y}, v_{\epsilon z}\}$	=	velocity components in $\mathcal{T}_\epsilon$, [km/s]
w	=	auxiliary variable
α	=	sail cone angle, [deg]
β	=	lightness number
δ	=	sail clock angle, [deg]
θ	=	azimuth angle, [deg]
$\mu_\odot$	=	Sun's gravitational parameter, [km^3/s^2]
ν	=	true anomaly, [deg]
τ	=	dimensionless time
ϕ	=	elevation angle, [deg]
Ω	=	right ascension of the ascending node, [deg]
ω	=	argument of pericenter, [deg]

Subscripts

0	=	initial value, parking orbit
t	=	final value, target orbit

Superscripts

$\cdot$	=	derivative with respect to time
$'$	=	derivative with respect to τ
$\sim$	=	estimate

1. Introduction

Long mission times are usually necessary to complete a heliocentric transfer with a solar sail, due to the small thrust level that may be got from such a propulsion system [12]. Not surprisingly, a solar sail trajectory is therefore often studied within an optimal framework, by looking for the control law that minimizes the total transfer time. In that context, optimization methods are mostly divided into two categories, either indirect or direct methods [5]. The indirect approach uses the calculus of variations and the Pontryagin's maximum principle to formulate a two-point boundary value problem, whose solution gives the optimal control law [27]. However, the high sensitivity of costates to their initial guess often prevents this method from obtaining a feasible solution [11] . On the other hand, direct methods translate a continuous optimal control problem into a nonlinear programming problem, which requires an initial guess of the optimal trajectory to compute the minimum-time solution [2]. In any case, both approaches are usually expensive in terms of computational costs [4], to such an extent that the simulation times are hardly manageable for preliminary mission analyses and feasibility assessment.

For this reason, many methods exist to generate fast approximations of spacecraft trajectories. A largely used technique is the so-called shape-based method, in which the shape of the trajectory is a priori described by a given function [21, 32, 31]. In that case, a set of parameters must be tuned to get a feasible solution, able to meet the boundary constraints. In this regard, [9] have developed a method based on the concept of Bezier curve functions to design three-dimensional heliocentric trajectories of a spacecraft equipped with an Electric Solar Wind Sail [10, 16]. [20] have proposed a shape-based approach to obtain an approximate solar sail trajectory to be used as a first guess solution for a multiple-asteroid rendezvous optimization problem. [28, 29] have used finite Fourier series to shape the position coordinates of a spacecraft with a low-thrust

propulsion system, whose thrust vector can be freely oriented in the space. In particular, their approximated trajectory was obtained by solving an optimization problem in which the cost function is the total velocity variation.

This paper proposes a procedure similar to the method developed by [29] to get an approximate optimal trajectory for a solar sail-based spacecraft in a heliocentric mission scenario, but also takes into account the physical constraints related to the fact that the sail thrust vector cannot be oriented toward the Sun. The spacecraft position along its parking and target orbits is not fixed, but is an output of the optimization process, in order to obtain an optimal orbit-to-orbit (heliocentric) transfer. The proposed method is validated in both a two- and a three-dimensional Earth-Mars transfer, and also using a more complex case, in which the sail is to be transferred to a near-Earth asteroid [35] . A comparison is eventually made with the numerical results obtained using an indirect approach [14, 15, 34, 19, 17] .

2. Mathematical preliminaries

Consider a spacecraft propelled by a solar sail, which must be transferred from an initial heliocentric parking orbit (subscript 0) of given characteristics $\{a_0, e_0, i_0, \Omega_0, \omega_0\}$, to a target orbit (subscript t) with parameters $\{a_t, e_t, i_t, \Omega_t, \omega_t\}$, where a is the semimajor axis, e is the eccentricity, i is the inclination, Ω is the right ascension of the ascending node, and ω is the argument of pericenter. Assuming the spacecraft to be subjected only to the Sun's gravitational attraction and to the sail propulsive acceleration $\boldsymbol{a}$, its equation of motion is

$$\ddot{\boldsymbol{r}} = -\frac{\mu_\odot}{r^3}\boldsymbol{r} + \boldsymbol{a} \tag{1}$$

where $\mu_\odot$ is the Sun's gravitational parameter, $\boldsymbol{r}$ is the Sun-spacecraft position vector, and $r = \|\boldsymbol{r}\|$ is the solar distance. Introduce now an inertial heliocentric-ecliptic reference frame $\mathcal{T}_\epsilon(O; x_\epsilon, y_\epsilon, z_\epsilon)$, whose origin O coincides with the Sun's center-of-mass, x_ϵ points toward the vernal equinox Υ, and z_ϵ is orthogonal to the ecliptic plane. Consider also the spherical coordinate system $\mathcal{T}_s(O; r, \theta, \phi)$ illustrated in Fig. 1, where θ is the angle between the x_ϵ-axis and the projection of $\boldsymbol{r}$ on the ecliptic, while ϕ is the angle between the ecliptic and the spacecraft position vector $\boldsymbol{r}$. Figure 1 also shows the unit vector $\hat{\boldsymbol{e}}_r$ along the radial direction, while

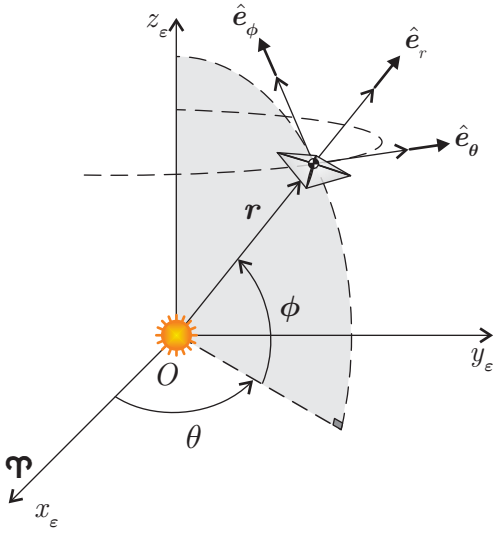

Figure 1: Heliocentric-ecliptic $\mathcal{T}_\epsilon(O; x_\epsilon, y_\epsilon, z_\epsilon)$, and spherical $\mathcal{T}_s(O; r, \theta, \phi)$ reference frame.

$\hat{\boldsymbol{e}}_\theta$ and $\hat{\boldsymbol{e}}_\phi$ are defined along the direction of the azimuth angle θ and the elevation angle ϕ, respectively.

Equation (1) may equivalently be rewritten as a system of three scalar differential equations, that is

$$\ddot{r} - r\,\dot{\theta}^2\,\cos^2\phi - r\,\dot{\phi}^2 = -\frac{\mu_\odot}{r^2} + a_r \tag{2}$$

$$2\,\dot{r}\,\dot{\theta}\,\cos\phi + r\,\ddot{\theta}\,\cos\phi - 2\,r\,\dot{\theta}\,\dot{\phi}\,\sin\phi = a_\theta \tag{3}$$

$$2\,\dot{r}\,\dot{\phi} + r\,\dot{\theta}^2\,\cos\phi\,\sin\phi + r\,\ddot{\phi} = a_\phi \tag{4}$$

where a_r, a_θ, and a_ϕ are the components of the propulsive acceleration vector $\boldsymbol{a}$ along $\hat{\boldsymbol{e}}_r$, $\hat{\boldsymbol{e}}_\theta$, and $\hat{\boldsymbol{e}}_\phi$, respectively. Assuming a flat sail model without degradation effects [7, 6], and using the optical force model described by [33] and [13], the propulsive acceleration vector $\boldsymbol{a}$ may be written as

$$\boldsymbol{a} = \frac{\beta\,\mu_\odot}{2\,r^2}\left(\hat{\boldsymbol{n}}\cdot\hat{\boldsymbol{e}}_r\right)\left[b_1\hat{\boldsymbol{e}}_r + (b_2\hat{\boldsymbol{n}}\cdot\hat{\boldsymbol{e}}_r + b_3)\hat{\boldsymbol{n}}\right] \tag{5}$$

where $\hat{\boldsymbol{n}}$ is the unit vector normal to the sail plane in the direction opposite to the Sun, $\{b_1, b_2, b_3\}$ are the dimensionless force coefficients [14], and β is the sail lightness number, defined as

$$\beta = \frac{2}{b_1 + b_2 + b_3}\left(\frac{a_c}{a_\oplus}\right) \tag{6}$$

where $a_\oplus \simeq 5.93\,\mathrm{mm/s^2}$ is the Sun's gravitational acceleration at the reference distance $r = r_\oplus \triangleq 1\,\mathrm{au}$, and a_c is the spacecraft characteristic acceleration, that is, the propulsive acceleration magnitude $\|\boldsymbol{a}\|$ of a Sun-facing sail when $r = r_\oplus$. According to [8], the values of the sail force coefficients used in the following discussion are $b_1 = 0.1901$, $b_2 = 1.6198$ and $b_3 = 0.0299$, based on recent experimental tests conducted on a thin polymer sail (with a thickness of 2.5 micrometer), coated with 10 nanometers of aluminum on the front side and with an uncoated back side.

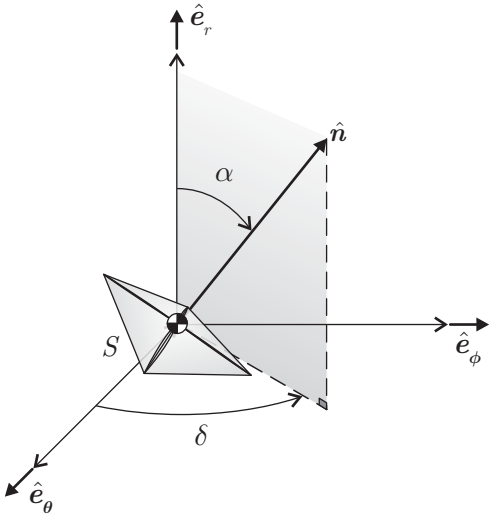

Figure 2: Cone (α) and clock (δ) angle.

From Eq. (5), the components of the propulsive acceleration vector are

$$a_r = \boldsymbol{a}\cdot\hat{\boldsymbol{e}}_r = \frac{\beta\,\mu_\odot}{2\,r^2}\left(b_1\cos\alpha + b_2\cos^3\alpha + b_3\cos^2\alpha\right) \tag{7}$$

$$a_\theta = \boldsymbol{a}\cdot\hat{\boldsymbol{e}}_\theta = \frac{\beta\,\mu_\odot}{2\,r^2}\left(b_2\cos\alpha + b_3\right)\cos\alpha\,\sin\alpha\,\cos\delta \tag{8}$$

$$a_\phi = \boldsymbol{a}\cdot\hat{\boldsymbol{e}}_\phi = \frac{\beta\,\mu_\odot}{2\,r^2}\left(b_2\cos\alpha + b_3\right)\cos\alpha\,\sin\alpha\,\sin\delta \tag{9}$$

where $\alpha \in [0, 90]$ deg is the sail cone angle, defined as the angle between the unit vectors $\hat{\boldsymbol{e}}_r$ and $\hat{\boldsymbol{n}}$, whereas $\delta \in [-180, 180)$ deg is the clock angle, that is, the angle between $\hat{\boldsymbol{e}}_\theta$ and the projection of $\hat{\boldsymbol{n}}$ on the plane $\{\hat{\boldsymbol{e}}_\theta, \hat{\boldsymbol{e}}_\phi\}$; see Fig. 2.

The aim of this work is to compute the minimum-time trajectory necessary to transfer a spacecraft between two given heliocentric orbits. The spacecraft position along the initial and the final orbit is not fixed, but is an output of the optimization process. The initial (or final) spacecraft state may be expressed as a function of the azimuth angle θ_0 (or θ_t) at the initial (or final) time, while the true anomaly ν_0 (or ν_t) is obtained with the procedure discussed in the following section.

2.1. Boundary conditions

With reference to Fig. 3, consider the spherical triangle obtained by intersecting three unitary circles, along the ecliptic plane, the meridian plane containing the sail and the orbital plane. Upon applying the spherical law of cosines to the angles of such a triangle, it is found that

$$\cos\gamma = \sin i \, \cos(\theta - \Omega) \tag{10}$$

$$\sin\gamma = \sqrt{1 - \cos^2\gamma} = \sqrt{1 - \sin^2 i \, \cos^2(\theta - \Omega)} \tag{11}$$

$$\cos i = \sin\gamma \, \cos\phi. \tag{12}$$

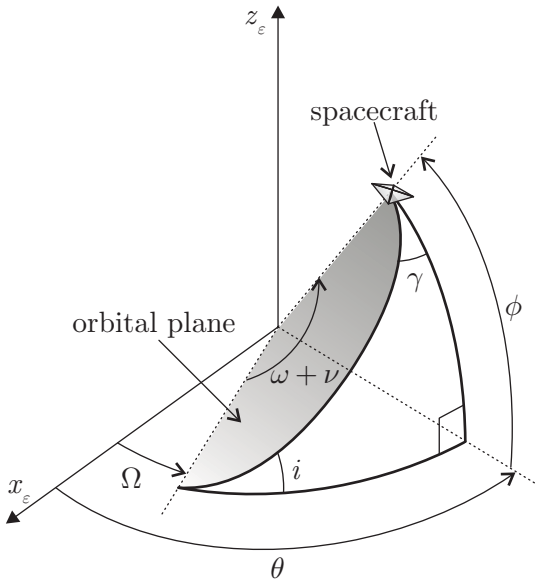

Figure 3: Spherical triangle.

Moreover, using the sine rule

$$\frac{\sin\phi}{\sin i} = \frac{\sin(\theta - \Omega)}{\sin\gamma} = \sin(\omega + \nu) \tag{13}$$

from which $\sin\phi$ and $\cos\phi$ are obtained as

$$\sin\phi = \frac{\sin(\theta - \Omega)\sin i}{\sqrt{1 - \sin^2 i \, \cos^2(\theta - \Omega)}} \quad , \quad \cos\phi = \frac{\cos i}{\sqrt{1 - \sin^2 i \, \cos^2(\theta - \Omega)}}. \tag{14}$$

Finally, bearing in mind Eqs. (11) and (13) and using the cosine rule for the sides, we get

$$\sin(\omega + \nu) = \frac{\sin(\theta - \Omega)}{\sqrt{1 - \sin^2 i \, \cos^2(\theta - \Omega)}} \quad , \quad \cos(\omega + \nu) = \frac{\cos(\theta - \Omega)\cos i}{\sqrt{1 - \sin^2 i \, \cos^2(\theta - \Omega)}}. \tag{15}$$

The latter two relations allow the true anomaly ν to be obtained as a function of the azimuth angle θ.

Note that, when the true anomalies ν_0 and ν_t along the initial and final orbits are known, the initial and final states of the spacecraft are fully defined. Indeed, according to [1], the components of the position and velocity vectors in $\mathcal{T}_\epsilon$ may be obtained as functions of the orbital parameters. These same components may also be expressed with respect to the spherical coordinate frame $\mathcal{T}_s$ as

$$r = \sqrt{x_\epsilon^2 + y_\epsilon^2 + z_\epsilon^2} \tag{16}$$

$$\phi = \arcsin\left(\frac{z_\epsilon}{\sqrt{x_\epsilon^2 + y_\epsilon^2 + z_\epsilon^2}}\right) \tag{17}$$

$$v_r = v_{\epsilon x}\frac{x_\epsilon}{r} + v_{\epsilon y}\frac{y_\epsilon}{r} + v_{\epsilon z}\frac{z_\epsilon}{r} \tag{18}$$

$$v_\theta = -v_{\epsilon x}\frac{y_\epsilon}{\sqrt{x_\epsilon^2 + y_\epsilon^2}} + v_{\epsilon y}\frac{x_\epsilon}{\sqrt{x_\epsilon^2 + y_\epsilon^2}} \tag{19}$$

$$v_\phi = -v_{\epsilon x}\frac{x_\epsilon z_\epsilon}{r\sqrt{x_\epsilon^2 + y_\epsilon^2}} - v_{\epsilon y}\frac{y_\epsilon z_\epsilon}{r\sqrt{x_\epsilon^2 + y_\epsilon^2}} + v_{\epsilon z}\frac{\sqrt{x_\epsilon^2 + y_\epsilon^2}}{r} \tag{20}$$

where $\{x_\epsilon, y_\epsilon, z_\epsilon\}$ (or $\{v_{\epsilon x}, v_{\epsilon y}, v_{\epsilon z}\}$) are the components of the spacecraft position (or velocity) vector in the heliocentric ecliptic reference frame, while $\{v_r, v_\theta, v_\phi\}$ are the velocity vector components in the spherical reference frame.

3. Finite Fourier series approximation

An approximation of the optimal three-dimensional trajectory of a solar sail can be obtained by shaping it with a classical finite Fourier series. To that end, the time variation of the generic spacecraft state variable $f \in \{r, \theta, \phi\}$ can be expressed as

$$f(\tau) = \frac{b_{f0}}{2} + \sum_{n=1}^{N_c}\left[b_{fn}\cos(n\pi\tau) + c_{fn}\sin(n\pi\tau)\right] \tag{21}$$

where $\tau \triangleq t/t_f \in [0, 1]$ is the dimensionless time (t_f is the total flight time), and $N_c \geq 2$ is the number of Fourier coefficients $\{b_{fn}, c_{fn}\}$. In particular, the first and second derivatives of f with respect to τ are

$$f'(\tau) = \sum_{n=1}^{N_c}\left[-b_{fn}n\pi\sin(n\pi\tau) + c_{fn}n\pi\cos(n\pi\tau)\right] \tag{22}$$

$$f''(\tau) = \sum_{n=1}^{N_c}\left[-b_{fn}(n\pi)^2\cos(n\pi\tau) - c_{fn}(n\pi)^2\sin(n\pi\tau)\right]. \tag{23}$$

Paralleling the procedure described by [29], some of the Fourier coefficients can be expressed as functions of the initial (at $\tau = 0$) and final (at $\tau = 1$) conditions, viz.

$$b_{f1} = \frac{f(0) - f(1)}{2} + \sum_{n=3}^{N_c} \left[\frac{(-1)^n - 1}{2} \right] b_{fn} \tag{24}$$

$$b_{f2} = \frac{f(0) + f(1)}{2} - \frac{b_{f0}}{2} - \sum_{n=3}^{N_c} \left[\frac{1 + (-1)^n}{2} \right] b_{fn} \tag{25}$$

$$c_{f1} = \frac{f'(0) - f'(1)}{2\pi} + \sum_{n=3}^{N_c} n \left[\frac{(-1)^n - 1}{2} \right] c_{fn} \tag{26}$$

$$c_{f2} = \frac{f'(0) + f'(1)}{4\pi} - \sum_{n=3}^{N_c} n \left[\frac{1 + (-1)^n}{4} \right] c_{fn}. \tag{27}$$

Observing that the derivative with respect to τ can be written as

$$\frac{\mathrm{d}f}{\mathrm{d}\tau} = t_f \frac{\mathrm{d}f}{\mathrm{d}t} \tag{28}$$

then

$$r' = t_f \dot{r} = t_f v_r \tag{29}$$

$$\theta' = t_f \dot{\theta} = t_f \frac{v_\theta}{r \cos\phi} \tag{30}$$

$$\phi' = t_f \dot{\phi} = t_f \frac{v_\phi}{r}. \tag{31}$$

Substituting Eqs. (24)–(27) into Eq. (21), the result is

$$f(\tau) = C_f + C_{bf0} b_{f0} + \sum_{n=3}^{N_c} \left(C_{bfn} b_{fn} + C_{cfn} c_{fn} \right) \tag{32}$$

with

$$f'(\tau) = C'_f + C'_{bf0} b_{f0} + \sum_{n=3}^{N_c} \left(C'_{bfn} b_{fn} + C'_{cfn} c_{fn} \right) \tag{33}$$

$$f''(\tau) = C''_f + C''_{bf0} b_{f0} + \sum_{n=3}^{N_c} \left(C''_{bfn} b_{fn} + C''_{cfn} c_{fn} \right) \tag{34}$$

where

$$C_f = \frac{f(0)-f(1)}{2}\cos(\pi\tau) + \frac{f(0)+f(1)}{2}\cos(2\pi\tau) + \\ + \frac{f'(0)-f'(1)}{2\pi}\sin(\pi\tau) + \frac{f'(0)+f'(1)}{4\pi}\sin(2\pi\tau) \tag{35}$$

$$C_{bf0} = \frac{1}{2}\big[1-\cos(2\pi\tau)\big] \tag{36}$$

$$C_{bfn} = \frac{(-1)^n-1}{2}\cos(\pi\tau) - \frac{1+(-1)^n}{2}\cos(2\pi\tau) + \cos(n\pi\tau) \tag{37}$$

$$C_{cfn} = n\frac{(-1)^n-1}{2}\sin(\pi\tau) - n\frac{1+(-1)^n}{4}\sin(2\pi\tau) + \sin(n\pi\tau). \tag{38}$$

It is now necessary to find the coefficients b_{f0}, b_{fn} and c_{fn} that describe the optimal (minimum-time) transfer trajectory.

4. Optimization procedure

The problem consists in determining the minimum-time trajectory that transfers a solar sail-based spacecraft from an initial parking orbit toward a final target orbit. Approximating the spacecraft position coordinates with Eq. (32), the control parameters of the optimization problem are the coefficients $\{b_{f0}, b_{fn}, c_{fn}\}$ of the finite Fourier series, the initial and final azimuth angles $\{\theta_0, \theta_t\}$, and the flight time t_f. Recall from the previous discussion that, as long as $N_c \geq 2$, the coefficients $\{b_{f1}, b_{f2}, c_{f1}, c_{f2}\}$ are functions of the initial and final conditions. Therefore, the total number of unknown parameters is $N_u = 6\,N_c - 6$.

The components of the propulsive acceleration vector may be related to the control variables through Eqs. (2)–(4) and (32)–(34) as

$$a_r = \frac{1}{t_f^2}\left[r'' - r\theta'^2\cos^2\phi - r\phi'^2\right] + \frac{\mu_\odot}{r^2} \tag{39}$$

$$a_\theta = \frac{1}{t_f^2}\left[2r'\theta'\cos\phi + r\theta''\cos\phi - 2r\theta'\phi'\sin\phi\right] \tag{40}$$

$$a_\phi = \frac{1}{t_f^2}\left[2r'\phi' + r\theta'^2\cos\phi\sin\phi + r\phi''\right]. \tag{41}$$

Suitable constraints have to be enforced on the magnitude and direction of the solar sail acceleration vector $\boldsymbol{a}$. In fact, the radial component of $\boldsymbol{a}$ must be positive, that is

$$a_r \geq 0 \tag{42}$$

while its magnitude must satisfy the following equation

$$\|\boldsymbol{a}\|^2 = a_r^2 + a_\theta^2 + a_\phi^2 = \\ = \left(\frac{\beta\mu}{2r^2}\right)^2\left[(b_1 + b_2\cos^2\alpha + b_3\cos\alpha)^2\cos^2\alpha + (b_2\cos^2\alpha + b_3\cos\alpha)^2\sin^2\alpha\right] \tag{43}$$

where the right-hand side comes from Eqs. (7)–(9), whereas α is obtained from Eq. (7), which may be rewritten as

$$\cos^3\alpha + a_2\cos^2\alpha + a_1\cos\alpha + a_0 = 0 \tag{44}$$

with

$$a_0 \triangleq -\frac{2r^2 a_r}{\beta \mu_\odot b_2} \quad , \quad a_1 \triangleq \frac{b_1}{b_2} \quad , \quad a_2 \triangleq \frac{b_3}{b_2}. \tag{45}$$

Equation (44) is a cubic polynomial equation in $\cos\alpha$. It may be solved in closed form by introducing the auxiliary variable s such that

$$\cos\alpha \triangleq s - \frac{a_2}{3}. \tag{46}$$

In fact, substituting Eq. (46) into Eq. (44), the latter reduces to

$$s^3 + q_1 s = q_2 \tag{47}$$

where

$$q_1 \triangleq \frac{3a_1 - a_2^2}{3} \quad , \quad q_2 \triangleq \frac{9a_1 a_2 - 27a_0 - 2a_2^3}{27}. \tag{48}$$

Note that, from Eq. (45), q_1 can also be written as

$$q_1 = a_1 - \frac{1}{3}a_2^2 \equiv \frac{b_1}{b_2} - \frac{1}{3}\left(\frac{b_3}{b_2}\right)^2. \tag{49}$$

Using the definition of sail force coefficients given by [14] and considering their typical values [8], it follows that $|b_3| < b_1$ and $b_2 > 0$. Therefore, the value of q_1 is positive. For example, when $b_1 = 0.1901$, $b_2 = 1.6198$ and $b_3 = 0.0299$, it follows that $q_1 \simeq 0.1172$. Introduce now a second auxiliary variable w defined as

$$s \triangleq w - \frac{q_1}{3w}. \tag{50}$$

Substituting Eq. (50) into Eq. (47), resulting sixth-order equation is

$$w^6 - q_2 w^3 - \frac{q_1^3}{27} = 0 \tag{51}$$

which has two pairs of complex conjugate solutions and two real solutions given by

$$w_{1,2} = \left[\frac{1}{2}\left(q_2 \pm \sqrt{q_2^2 + \frac{4}{27}q_1^3}\right)\right]^{\frac{1}{3}}. \tag{52}$$

It may be easily checked that the same value of s is obtained when either w_1 or w_2 is substituted into Eq. (50). Such a value of s can be used in Eq. (46) to get the actual value of $\cos\alpha$.

To solve this optimization problem, the whole time domain is discretized into N_p Legendre-Gauss nodes, and a nonlinear programming solver is used to obtain the set of control variables that minimize the flight time t_f. In particular, the interior-point method implemented in the MATLAB built-in function `fmincon` has been used. Note that an initial solution guess is required to run the interior-point algorithm. To that end, using the procedure suggested by [29], the spacecraft states $\{r, \theta, \phi\}$ can be approximated with a cubic polynomial expression in the form

$$\widetilde{f}(\tau) = c_0 + c_1\tau + c_2\tau^2 + c_3\tau^3 \tag{53}$$

whose parameters $\{c_0, c_1, c_2, c_3\}$ are obtained by enforcing the boundary conditions involving $f(0)$, $f(1)$, $f'(0)$, and $f'(1)$. Equation (53) is then evaluated at the nodes, and the Fourier series coefficients are calculated with a fitting procedure.

An estimate of the flight time $\widetilde{t}_f$ may be found with the approximate analytical expression by [23], which is valid for a circle-to-circle orbit raising (or lowering) when the solar sail characteristic acceleration is sufficiently small. Otherwise, an initial guess of $\widetilde{t}_f$ can be obtained as the ratio of the magnitude of the angular momentum vector change to the torque induced by the solar sail propulsive acceleration [9], viz.

$$\widetilde{t}_f = \frac{\sqrt{\mu_\odot(p_0 + p_t) - 2\mu_\odot\sqrt{p_0 p_t}\cos(i_t - i_0)}}{\widetilde{r}\,(\beta\mu_\odot)/(2\widetilde{r}^2)\,(b_2\cos\alpha_{\max} + b_3)\cos\alpha_{\max}\sin\alpha_{\max}} \tag{54}$$

where $\widetilde{r} = (a_0 + a_t)/2$, p is the semilatus rectum, and $\alpha_{\max} \simeq 35.2\,\text{deg}$ is the sail cone angle that maximizes the transverse component of the solar sail propulsive acceleration. Finally, the initial guesses of the two azimuth angles $\{\theta_0, \theta_t\}$ are chosen by a trial and error procedure.

5. Mission scenarios and numerical simulations

The procedure described in the previous sections is now applied to the optimization problem of an Earth-Mars orbit-to-orbit transfer in a simplified two-dimensional case and in a more realistic three-dimensional scenario. It is also applied to a transfer toward the near-Earth (potentially hazardous) asteroid 1620 Geographos. In all of the simulations, a solar sail with a canonical value [13] of characteristic acceleration ($a_c = 1\,\mathrm{mm/s^2}$) is considered, while the number of Fourier coefficients is $N_c = 10$.

5.1. Two-dimensional simplified Earth-Mars transfer

Consider first a simplified, two-dimensional, Earth-Mars interplanetary transfer, in which the solar sail-based spacecraft initially covers an orbit coinciding with that of the Earth (with orbital parameters $a_0 = 1\,\mathrm{au}$, $e_0 = 0.0167$, $i_0 = 0$, and $\Omega_0 + \omega_0 = 102.95\,\mathrm{deg}$), and must be transferred toward a target coplanar orbit of parameters $a_t = 1.524\,\mathrm{au}$, $e_t = 0.0934$, $i_t = 0$, and $\Omega_t + \omega_t = 336.04\,\mathrm{deg}$. Note that the target orbit is consistent with the Mars heliocentric orbit when its orbital inclination is set equal to zero.

In a two-dimensional case, the constraints on the elevation angle and its derivatives with respect to τ are

$$\phi = 0 \quad , \quad \phi' = 0 \quad , \quad \phi'' = 0 \tag{55}$$

and the Fourier coefficients $\{b_{\phi 0}, b_{\phi n}, c_{\phi n}\}$ are

$$b_{\phi 0} = 0 \quad , \quad b_{\phi n} = 0 \quad , \quad c_{\phi n} = 0. \tag{56}$$

Substituting Eq. (55) into Eqs. (39)–(41), the components of the sail propulsive acceleration become

$$a_r = \frac{1}{t_f^2}\left[r'' - r\theta'^2\right] + \frac{\mu_\odot}{r^2} \tag{57}$$

$$a_\theta = \frac{1}{t_f^2}\left[2r'\theta' + r\theta''\right] \tag{58}$$

$$a_\phi = 0. \tag{59}$$

The unknown parameters are the Fourier coefficients $\{b_{r0}, b_{rn}, c_{rn}, b_{\theta 0}, b_{\theta n}, c_{\theta n}\}$, the azimuth angles $\{\theta_0, \theta_t\}$, and the flight time t_f. The time domain is discretized into $N_p = 20$ Legendre-Gauss nodes, and the optimization procedure gives a flight time $t_f \simeq 379.9\,\mathrm{days}$. The corresponding transfer trajectory is shown in Fig. 4. In this case, the initial and final azimuth angles are $\theta_0 \simeq 234.9\,\mathrm{deg}$ and $\theta_t \simeq 472.4\,\mathrm{deg}$. Figure 5

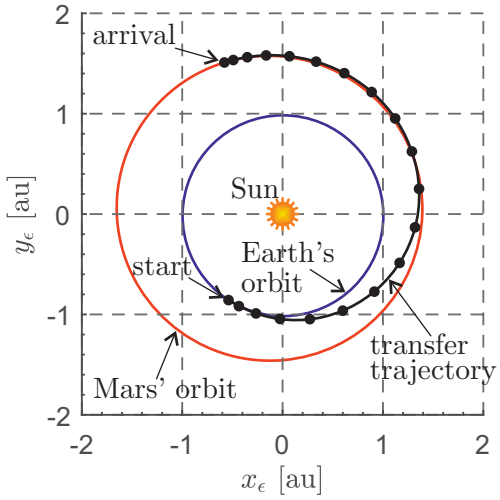

Figure 4: Earth-Mars optimal two-dimensional transfer trajectory when $a_c = 1\ \mathrm{mm/s^2}$, with $N_p = 20$ and $N_c = 10$.

illustrates the optimal control law $\alpha = \alpha(\tau)$, while $\delta(\tau) = 0$ because the problem is two-dimensional. Figures 4-5 also show the position of the nodes (represented by circles) at which the constraints given by Eqs. (42)-(43) are enforced.

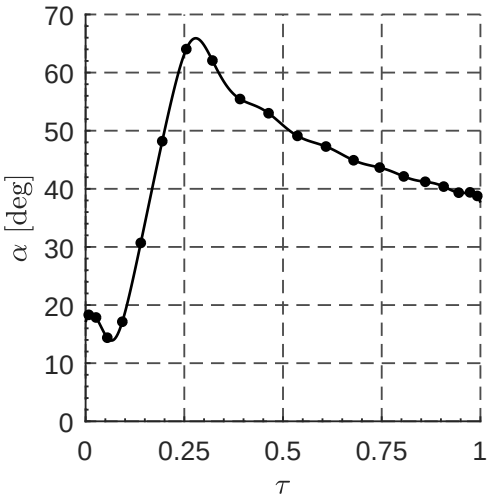

Figure 5: Optimal control law $\alpha = \alpha(\tau)$ for an Earth-Mars two-dimensional transfer when $a_c = 1$ mm/s^2, with $N_p = 20$ and $N_c = 10$.

5.2. Three-dimensional Earth-Mars transfer

A three-dimensional case is now investigated. The Earth's (parking) orbital parameters are $a_0 = 1\,\text{au}$, $e_0 = 0.0167$, $i_0 = 0$, $\Omega_0 = 348.74\,\text{deg}$, $\omega_0 = 114.21\,\text{deg}$, while those of Mars are $a_t = 1.524\,\text{au}$, $e_t = 0.0934$, $i_t = 1.85\,\text{deg}$, $\Omega_t = 49.58\,\text{deg}$, $\omega_t = 286.46\,\text{deg}$.

The values of θ_0, θ_t and t_f obtained in the two-dimensional scenario are used as initial guesses to solve the three-dimensional case. The minimum flight time t_f and the optimal values of the azimuth angles $\{\theta_0, \theta_t\}$ are shown in Tab. 1 as a function of the number of nodes $N_p = \{20, 25, 30, 35\}$, when $N_c = 10$. The optimal solution computed with an indirect approach gives a minimum flight time of about 382 days

N_p	t_f (days)	θ_0 (deg)	θ_t (deg)
20	383.30	229.20	469.79
25	383.23	229.89	470.42
30	383.18	229.99	470.47
35	383.12	230.43	470.89

Table 1: Minimum flight time t_f, optimal values of θ_0 and θ_t as a function of the number N_p of nodes, for an Earth-Mars transfer with $a_c = 1$ mm/s^2, when $N_c = 10$.

The minimum-time trajectory, computed using $N_p = 30$ nodes, is characterized by a total flight time $t_f \simeq 383.18\,\text{days}$, and is shown in Fig. 6. The optimal values of the initial and final azimuth angles are $\theta_0 \simeq 230\,\text{deg}$ and $\theta_t \simeq 470.5\,\text{deg}$. The optimal control laws $\alpha = \alpha(\tau)$ and $\delta = \delta(\tau)$, obtained with the Fourier series method with $N_p = 30$ nodes, are shown in Figs. 7(a)-7(b) with red solid line, and are compared to the optimal control laws obtained with an indirect approach [3, 14], reported with dashed black line. Figures 7(a) and 7(b) show that the Fourier series method is able to provide a good approximation of the actual optimal control laws.

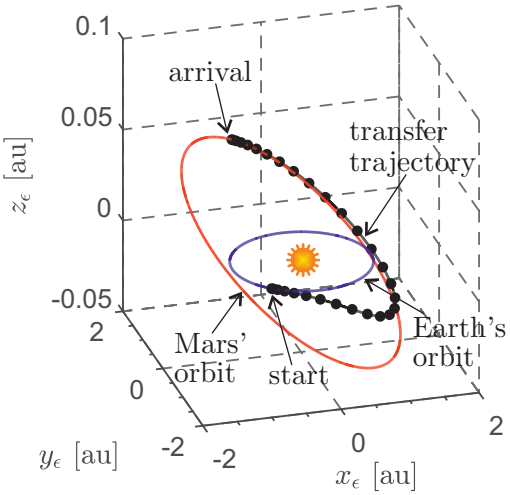

(a) Three-dimensional trajectory.

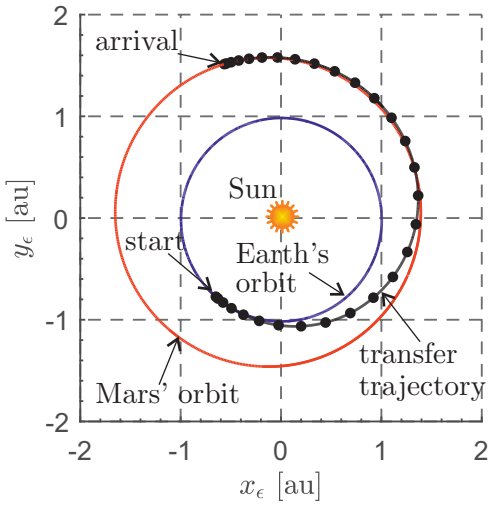

(b) Ecliptic projection.

Figure 6: Earth-Mars three-dimensional optimal transfer trajectory with $a_c = 1$ mm/s^2, when $N_p = 30$ and $N_c = 10$.

5.3. Transfer from Earth to asteroid 1620 Geographos

A more involved problem is represented by a transfer toward the near-Earth asteroid 1620 Geographos. Such an asteroid has been extensively observed [18] and studied in the past literature because of its collision possibility with the Earth, and to improve our knowledge about asteroid rotational motion and meteor stream generation [24, 25, 26, 30]. It has also been proposed as a potential candidate for a multi-asteroid tour mission [22].

In this case, the spacecraft is assumed to initially cover a parking orbit coinciding with that of the Earth, whereas the orbital parameters of the target asteroid are $a_t = 1.2453$ au, $e_t = 0.3354$, $i_t = 13.3373$ deg, $\Omega_t = 337.19539$ deg, $\omega_t = 276.91504$ deg. The optimal value of t_f, θ_0 and θ_t are shown in Tab. 2 as a function of the number of nodes N_p.

The optimal trajectory, calculated with $N_p = 20$ and shown in Fig. 8, requires a total flight time of about 394 days. The minimum-time solution computed with an indirect approach is characterized by a value of t_f equal to 393 days. Figure 9 shows a comparison between the optimal control laws obtained with the Fourier

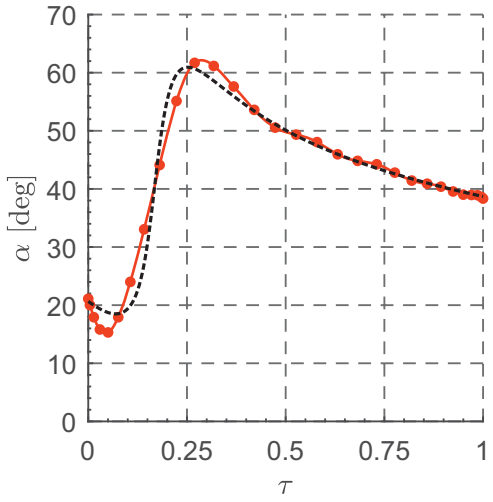

(a) Cone angle.

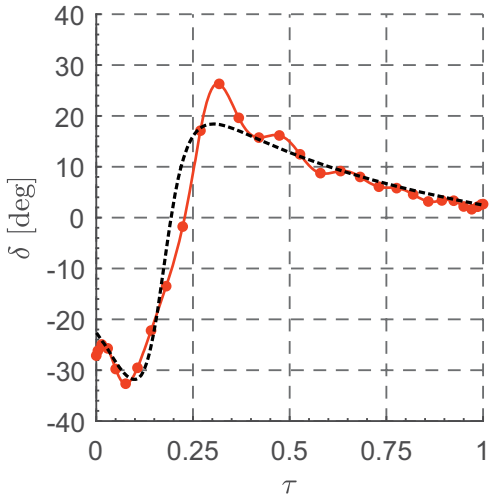

(b) Clock angle.

Figure 7: Time variation of the optimal control law for an Earth-Mars three-dimensional transfer when $a_c = 1$ mm/s^2, computed with Fourier series method with $N_p = 30$ and $N_c = 10$ (solid red line), and with an indirect approach (dashed black line).

N_p	t_f (days)	θ_0 (deg)	θ_t (deg)
20	393.56	338.39	721.69
25	393.23	336.99	720.67
30	393.13	334.13	718.45
35	393.01	335.40	720.59

Table 2: Minimum flight time t_f, optimal values of θ_0 and θ_t as a function of the number N_p of nodes, for an Earth-Geographos transfer with $a_c = 1$ mm/s^2, when $N_c = 10$.

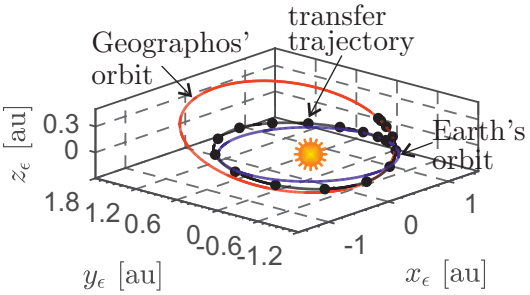

(a) Three-dimensional trajectory.

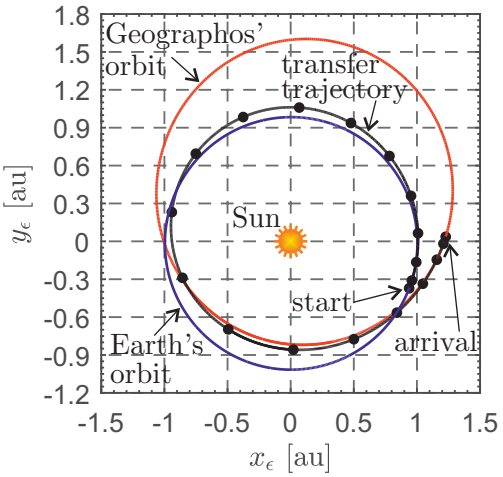

(b) Ecliptic projection.

Figure 8: Earth-Geographos optimal transfer trajectory when $a_c = 1$ mm/s^2, with $N_p = 20$ and $N_c = 10$.

series method (solid red line) and an indirect approach (dashed black line). Notably, the time-variations of the two control angles derived from the proposed approach are nearly coincident with the truly optimal solution that comes from an indirect method.

Note that, for the sake of conciseness, this section reports the results obtained with $N_c = 10$ only. In fact, this case gives the solutions closer to that obtained with an indirect approach. Further numerical simulations have shown that when either $N_c < 8$ or the number of nodes N_p is smaller than 20, the proposed method converges towards a solution with a longer flight time or to unfeasible points. These numbers are however not universal, since the best range of values of N_c and N_p may depend on the mission type considered in the study.

Due to its capability to produce an accurate approximation of the optimal trajectory with small computational efforts, the method presented in this paper may also be used to produce initial guess solutions for a more precise direct optimization method. In this context, it would be interesting to compare the performance of the Fourier series method with the procedure developed by [20] for generating an initial estimate for a direct approach. Extensive numerical simulations would be required to take into account different possible transfer scenarios and sail performance. An analysis of this problem is left to future research.

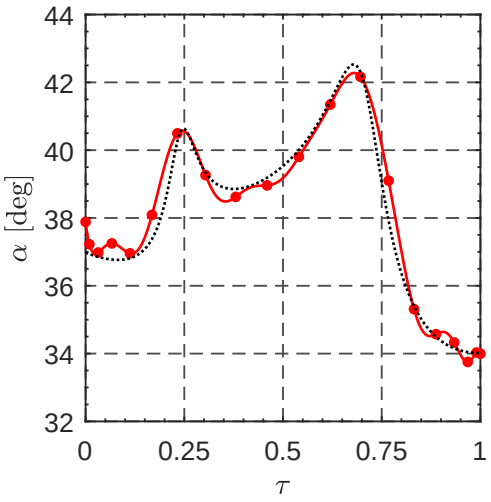

(a) Cone angle.

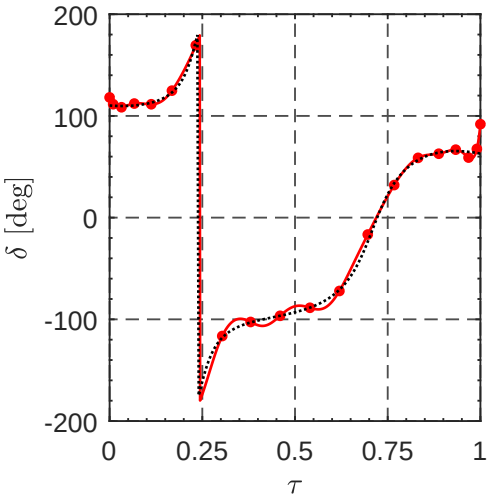

(b) Clock angle.

Figure 9: Time variation of the optimal control law for an Earth-Geographos transfer when $a_c = 1$ mm/s^2, computed with Fourier series method with $N_p = 20$ and $N_c = 10$ (solid red line), and with an indirect approach (dashed black line).

6. Conclusions

This paper has presented a method to obtain an approximate minimum-time trajectory for a solar sail-based spacecraft in a three-dimensional, heliocentric, mission scenario. The time variation of the generic spacecraft state is approximated by a finite Fourier series, and a suitable set of constraints are enforced on the magnitude and direction of the sail propulsive acceleration vector at the control points. The trajectory optimization problem consists in calculating the Fourier series coefficients that define the shape of the transfer trajectory.

The proposed method has been validated on two-dimensional and three-dimensional orbit-to-orbit transfer cases. The numerical results, when compared to those obtained using an indirect approach, show that the Fourier series-based method is able to provide a good approximation of the optimal trajectory and of

the minimum flight time, with a small computational effort. Due to its simplicity and effectiveness, the proposed procedure may be used either for a fast preliminary mission analysis or to provide an initial guess for a more refined direct optimization approach, in order to obtain an accurate solution of the minimum-time trajectory.

References

[1] Bate, R. R., Mueller, D. D., White, J. E., 1971. Fundamentals of Astrodynamics. Dover Publications, New York, Ch. 2, pp. 51–83, ISBN: 0-486-60061-0.

[2] Betts, J. T., Mar. 1998. Survey of numerical methods for trajectory optimization. Journal of Guidance, Control, and Dynamics 21 (2), 193–207, doi: 10.2514/2.4231.

[3] Bryson, A. E., Ho, Y. C., 1975. Applied Optimal Control. Hemisphere Publishing Corporation, New York, Ch. 2, pp. 71–89, ISBN: 0-891-16228-3.

[4] Caruso, A., Quarta, A. A., Mengali, G., Sep. 2019. Comparison between direct and indirect approach to solar sail circle-to-circle orbit raising optimization. Astrodynamics 3 (3), 273–284, doi: 10.1007/s42064-019-0040-x.

[5] Conway, B. A., Feb. 2012. A survey of methods available for the numerical optimization of continuous dynamic systems. Journal of Optimization Theory and Applications 152 (2), 271–306, doi: 10.1007/s10957-011-9918-z.

[6] Dachwald, B., Macdonald, M., McInnes, C. R., Mengali, G., Quarta, A. A., Jul. 2007. Impact of optical degradation on solar sail mission performance. Journal of Spacecraft and Rockets 44 (4), 740–749, doi: 10.2514/1.21432.

[7] Dachwald, B., Mengali, G., Quarta, A. A., Macdonald, M., Sep. 2006. Parametric model and optimal control of solar sails with optical degradation. Journal of Guidance, Control, and Dynamics 29 (5), 1170–1178, doi: 10.2514/1.20313.

[8] Heaton, A., Ahmed, N., Miller, K., Jan. 2017. Near earth asteroid scout thrust and torque model. Presentation at 4th International Symposium on Solar Sailing (ISSS 2017), Kyoto, Japan.

[9] Huo, M., Mengali, G., Quarta, A. A., Qi, N., May 2019. Electric sail trajectory design with bezier curve-based shaping approach. Aerospace Science and Technology 88, 126–135, doi: 10.1016/j.ast.2019.03.023.

[10] Janhunen, P., Jul. 2004. Electric sail for spacecraft propulsion. Journal of Propulsion and Power 20 (4), 763–764, doi: 10.2514/1.8580.

[11] Jiang, F., Baoyin, H., Li, J., Jan. 2012. Practical techniques for low-thrust trajectory optimization with homotopic approach. Journal of Guidance, Control, and Dynamics 35 (1), 245–258, doi: 10.2514/1.52476.

[12] Johnson, L., Young, R., Montgomery, E., Alhorn, D., 2011. Status of solar sail technology within NASA. Advances in Space Research 48 (11), 1687–1694, doi: 10.1016/j.asr.2010.12.011.

[13] McInnes, C. R., 1999. Solar Sailing: Technology, Dynamics and Mission Applications. Springer-Verlag Berlin, Ch. 2, pp. 46–51, ISBN: 978-1-85233-102-3.

[14] Mengali, G., Quarta, A. A., Jan. 2005. Optimal three-dimensional interplanetary rendezvous using nonideal solar sail. Journal of Guidance, Control, and Dynamics 28 (1), 173–177, doi: 10.2514/1.8325.

[15] Mengali, G., Quarta, A. A., Circi, C., Dachwald, B., Mar. 2007. Refined solar sail force model with mission application. Journal of Guidance, Control, and Dynamics 30 (2), 512–520, doi: 10.2514/1.24779.

[16] Mengali, G., Quarta, A. A., Janhunen, P., Jan. 2008. Electric sail performance analysis. Journal of Spacecraft and Rockets 45 (1), 122–129, doi: 10.2514/1.31769.

[17] Niccolai, L., Quarta, A. A., Mengali, G., Mar. 2017. Analytical solution of the optimal steering law for non-ideal solar sail. Aerospace Science and Technology 62, 11–18, doi: 10.1016/j.ast.2016.11.031.

[18] Ostro, S. J., Jurgens, R. F., Rosema, K. D., et al., May 1996. Radar observations of asteroid 1620 Geographos. Icarus 121 (1), 46–66, doi: 10.1006/icar.1996.0071.

[19] Pan, B., Lu, P., Pan, X., Ma, Y., 2016. Double-homotopy method for solving optimal control problems. Journal of Guidance, Control, and Dynamics 39 (8), 1706–1720, doi: 10.2514/1.G001553.

[20] Peloni, A., Ceriotti, M., Dachwald, B., 2016. Solar-sail trajectory design for a multiple near-earth-asteroid rendezvous mission. Journal of Guidance, Control, and Dynamics 39 (12), 2712–2724, doi: 10.2514/1.G000470.

[21] Petropoulos, A. E., Longuski, J. M., Sep. 2004. Shape-based algorithm for automated design of low-thrust, gravity-assist trajectories. Journal of Spacecraft and Rockets 41 (5), 787–796, doi: 10.2514/1.13095.

[22] Qiao, D., Cui, P., Cui, H., Aug. 2012. Proposal for a multiple-asteroid-flyby mission with sample return. Advances in Space Research 50 (3), 327–333, doi: 10.1016/j.asr.2012.04.014.

[23] Quarta, A. A., Mengali, G., Jan. 2012. Semi-analytical method for the analysis of solar sail heliocentric orbit raising. Journal of Guidance, Control, and Dynamics 35 (1), 330–335, doi: 10.2514/1.55101.

[24] Ryabova, G. O., 2002. Asteroid 1620 Geographos: I. rotation. Solar System Research 36 (2), 168–174, doi: 10.1023/A:1015226417427.

[25] Ryabova, G. O., 2002. Asteroid 1620 Geographos: II. associated meteor streams. Solar System Research 36 (3), 234–247, doi: 10.1023/A:1015897215612.

[26] Ryabova, G. O., 2004. Asteroid 1620 Geographos: III. inelastic relaxation in the vicinity of the poles. Solar System Research 38 (3), 212–218, doi: 10.1023/B:SOLS.0000030861.89529.18.

[27] Sauer, C. G., Aug. 1976. Optimum solar-sail interplanetary trajectories. Presentation at AIAA/AAS Astrodynamics Conference, San Diego, California.

[28] Taheri, E., Abdelkhalik, O., May 2012. Shape-based approximation of constrained low-thrust space trajectories using fourier series. Journal of Spacecraft and Rockets 49 (3), 535–545, doi: 10.2514/1.A32099.

[29] Taheri, E., Abdelkhalik, O., Feb. 2016. Initial three-dimensional low-thrust trajectory design. Advances in Space Research 57 (3), 889–903, doi: 10.1016/j.asr.2015.11.034.

[30] Ďurech, J., Vokrouhlický, D., Kaasalainen, M., et al., 2008. Detection of the YORP effect in asteroid (1620) Geographos. Astronomy and Astrophysics 489 (2), L25–L28, doi: 10.1051/0004-6361:200810672.

[31] Vellutini, E., Avanzini, G., Jul. 2014. Shape-based design of low-thrust trajectories to cislunar lagrangian point. Journal of Guidance, Control, and Dynamics 37 (4), 1329–1335, doi: 10.2514/1.G000165.
[32] Wall, B. J., Conway, B. A., Jan. 2009. Shape-based approach to low-thrust rendezvous trajectory design. Journal of Guidance, Control, and Dynamics 32 (1), 95–102, doi: 10.2514/1.36848.
[33] Wright, J. L., 1992. Space Sailing. Gordon and Breach Science Publishers, Philadelphia (USA), pp. 223–233, ISBN: 978-2881248429.
[34] Zeng, X., Alfriend, K. T., Vadali, S. R., Mar. 2014. Solar sail planar multireversal periodic orbits. Journal of Guidance, Control, and Dynamics 37 (2), 674–681, doi: 10.2514/1.58598.
[35] Zeng, X., Gong, S., Li, J., Dec. 2014. Fast solar sail rendezvous mission to near earth asteroids. Acta Astronautica 105 (1), 40–56, doi: 10.1016/j.actaastro.2014.08.023.